

INTERANNUAL VARIABILITY OF VEGETATION DYNAMICS IN THE SEMI-ARID NORTHEAST REGION OF BRAZIL AND ITS RELATIONSHIP TO ENSO EVENTS

Humberto Alves Barbosa¹

Fundação Cearense de Meteorologia e Recursos Hídricos - FUNCEME, Ceará, Brazil.

1. INTRODUCTION

The spatial-temporal analysis of the vegetation dynamics (i.e., the response of vegetation to climatic conditions) in the semi-arid tropical region is important to improve the climate modeling studies in simulating Sea Surface Temperature (SST)-dependent vegetation variability at climatic extremes (Cramer and Fischer, 1996). The Northeast region of Brazil (NEB) is the one such semi-arid tropical region suffering greatest impacts from climatic fluctuations caused by SST anomalies. Although studies have investigated the interannual relationships between SST anomalies and vegetation variations, few have attempted to examine the influence of SST on the semi-arid NEB vegetation during the last two decades of the 20th century.

Most of evidence presented by the recent studies on the influence of a strong El Niño-Southern Oscillation (ENSO) event on terrestrial ecosystems of NEB is qualitatively similar to those of the Southern Africa landscape (Azzali and Menenti, 2000). The large variations in rainfall, which cause either drought or (flooding), lead to either decrease or (increase) in land vegetation growth in this region, which are associated with the El Niño (drought) and La Niña (flooding) events. In many cases, however, there is a joint effect between the influence of a positive El Niño SST anomaly and positive gradient (North Atlantic warmer than South Atlantic), which tends to dramatically decrease rainfall during austral summer and autumn in the region (Alves and Repelli, 1992).

In the last two decades of the 20th century, the severity of occurrence of drought (meteorological) has grown over the increased frequency of ENSO events, which is asserted to be the fluctuation of the global atmospheric that is triggered by the SST anomalies occurring during ENSO events (Hulme, 2001). In particular, the period of 1991-1999 was marked by unusual El Niño activity that was developed in 1991 lasted almost continuously through 1995 and reappeared at record-

breaking levels in 1997, following a moderate La Niña in 1995-1996. However, it also seems that in the past, the environment was more resilient to changes in climate variability or extreme events in the NEB.

A few investigations have recently incorporated long time series of Normalized Difference Vegetation Index (NDVI) data taken by the National Oceanic and Atmospheric Administration (NOAA) Advanced Very High Resolution Radiometer (AVHRR) to monitor the dynamics of the spatial-temporal structures of vegetation systemic responses to the ENSO perturbations across the Brazilian semi-arid landscape (Barbosa et al., 2006; Barbosa, 2004; Dessay et al., 2004). The NOAA-AVHRR-NDVI, a normalized ratio of the near infrared (NIR) and red spectral light reflected (red) by the land surface back up into space $[(\text{NIR}-\text{red})/(\text{NIR}+\text{red})]$, is in fact linked to the presence, density and condition of vegetation and is also an indirect indicator of primary productivity through its linear relation with the percentage of absorbed photosynthetically active radiation (%APAR) (Curran, 1980). The raw NDVI values are fractional real numbers that range between -1 to +1 units, but when used to define the land cover classes, the values are normally constrained from + 0.1 units in deserts and up to + 0.8 units in dense tropical rainforest. There are also clear and positive linear relationships between NDVI and rainfall thanks to different analyses across the semi-arid tropical ecosystems (Nicholson et al., 1990) where rainfall is below an absolute amount of precipitation of 50-100 mm/month. This study gives an overview of a simple time series and composite analysis approaches to the interannual SST-dependent NEB NDVI modulation over the last two decades of the 20th century.

2. STUDY REGION

The spatial context for this study is carried in the Brazilian semi-arid region to investigate the influence of SST perturbations on

¹ Corresponding author address: Humberto Alves Barbosa
FUNCEME, Av. Rui Barbosa, 1246, Fortaleza, CE,
CEP:60115-221, Brazil E-Mail: barbosa@funceme.br

vegetation. The Brazilian semi-arid region is located within the NEB, approximately 1 to 18°S latitude and 35 to 47°W longitude (Fig. 1). NEB consists of nine states covering an area of about 1.5 million square kilometers. There is naturally a broad ecological variation in land cover types within the region where the prevalent environment is tropical semi-arid. The dynamics of this semi-arid tropical landscape are largely controlled by the timely onset of precipitation and its irregular distribution through the rainy season (February through May). Although precipitation variability for the NEB landscapes is the dominant factor controlling primary productivity, there is evidence that land degradation may affect the inter-relationships between vegetation and precipitation (Barbosa, 1998).

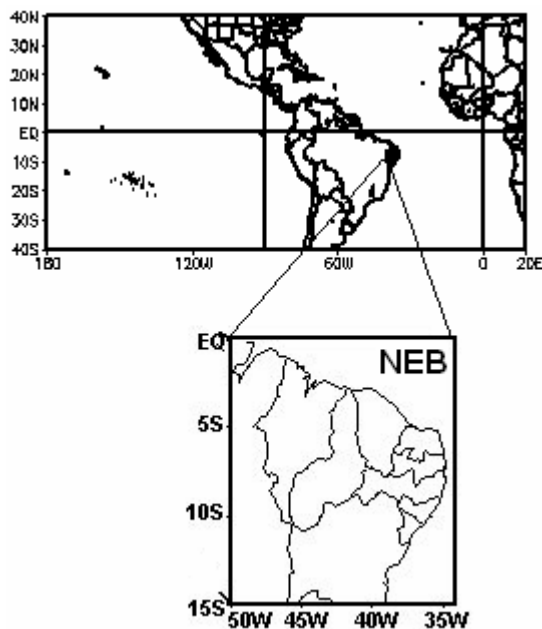


Fig. 1. Location of the Northeast Region of Brazil (NEB) in South America. The NEB extends over a land surface of approximately 1.5 million km², covering nine states in Brazil.

3. METHODOLOGY

Analyses performed in this study were based on the monthly NDVI imagery from the Goddard Distributed Active Archive Center (GDAAC) (ftp://daac.gsfc.nasa.gov/data/avhrr/continent/south_america/yearly, 2004); the file contains monthly mean analyzed SST from NOAA-CIRES Climate Diagnostics Center (CDC) (<http://www.cdc.noaa.gov>) and, Niño-3.4 and DIPOLE indices based on the SST anomalies from NOAA Climate Prediction Center (NOAA CPC) from 1982-2001. To describe SST teleconnections affecting NEB

terrestrial vegetation, a hemispheric scale domain of analysis is utilized and NEB NDVI gridded data are averaged over rainy season (from February to May) for the periods of 1980's and 1990's. NEB landscape conditions for the 1980's are contrasted with the 1990's by subtraction of the 1980's composite field from the 1990's. The aim is to assess the response of regional NEB terrestrial vegetation to SST fluctuations, and to consider which ENSO signal is present.

For the land cover data, the best candidate as a satellite NDVI data source is the Pathfinder Land (PAL) data base (PAL is a joint NOAA-NASA project). The monthly product from the PAL data base are produced at 8 km by 8 km pixel size resolution from NOAA Global Area Coverage (GAC) Level 1B data records and are available in the Goode Interrupted Homolosine map projection. The 20-year NDVI data were derived from four different NOAA satellites: (1) NOAA 7 from January 1982 to January 1985; (2) NOAA 9 from February 1985 to October 1988; (3) NOAA 11 from November 1988 to August 1994; and (4) NOAA 14 from January 1995 to September 2001. The author note that the NDVI data used here are monthly maximum value composite from the Pathfinder NOAA AVHRR data, which are also processed for various factors, including pre-launch calibration, intra sensor degradation, normalized for changes in solar zenith angle, and for Rayleigh scattering. The latter takes into consideration ozone absorption (using data from the Nimbus-7 Total Ozone Mapping Spectrometer (TOMS) and land surface elevation as used to correct the pressure level in order to determine Rayleigh coefficients. The SST data, which contain mean monthly SST fields and SST time series covering 1982-2001, comes from the best-track data collected continuously since 1947 by the NOAA-CIRES-CDC, currently located in Boulder, Colorado, from their Web site. These online data analysis are in the form of monthly mean fields and time series at a 2.5° latitude x 2.5° longitude resolution. Time series of monthly SST anomalies values used in this study are delimited by latitudes 170°W-120°W and longitudes 5°S-5°N (Niño-3.4 index), and also by the gradient between tropical North (5°N-25°N) and South Atlantic (5°S-25°S) (DIPOLE index).

Prior to statistical analyses, the 8-bit Pathfinder NDVI data were directly downloaded from GDAAC. The data were converted into NDVI value. For the entire study region (Fig. 1), Pathfinder data were processed to extract grid cell values for the period of interest. Mean 3 x 3 pixel arrays over the grids yielding a set of 12,000 spatially distributed NDVI values extracted for each month of the year for the

period of 1982-2001 (i.e., 240 months). Neither spatial interpolation methods nor correction for topographical features were employed. Monthly grids (12,000 NDVI values) were averaged to get spatially averaged NDVI value of each month. Finally, the averaged NDVI value per month over the whole grid (12,000 NDVI values) were used to facilitate statistical and analyses over time. The 240 values served as the reference standard for correlations with monthly mean SST fields from CDC.

The NDVI time series (NDVI 240 values) were then uploaded via FTP to a CDC public directory using anonymous FTP and they are read by a Perl script. The NEB NDVI time series were then correlated with time series for the SST fields for all locations using a linear correlation scheme provided at the CDC Web site. The results were regional correlation fields depicting regions of high and low correlation with the base locations fields. These regional correlations fields were used to help identify SST teleconnections. The correlation composite fields were created using GrADS batch scripts. Two concurrently reliable indicators were also considered; the Niño-3.4 index as an indicator of the ENSO and DIPOLE index as an indicator of the rainfall variability in the NEB (Moura and Shukla, 1981). The influence of these indices has been shown to exist on the interannual changes in the NEB rainfall, which are coupled to patterns of the equatorial Pacific SST (i.e., remote connections) and equatorial Atlantic Oceans (i.e., local connections). Thus, in this analysis the author focused on comparisons among NDVI patterns with the patterns of DIPOLE index. The author did, however, use mean-monthly values to calculate the characteristic DIPOLE and Niño-3.4 anomaly patterns. These means were based on the 1982-2001 period. In addition, the running averages were simply computed by averaging the 36 months from January 1982 through December 1984 that was plotted as the average of month 1, from February 1982 through January 1985 was plotted as the average of month 2, and so on. Scatter plots were employed to illustrate the results. Thus, in this study the methodology applied focuses on differences between composite field 1980's and 1990's, rather than comparisons with climatological patterns (30-yrs).

4. RESULTS

The monthly NEB NDVI and its 36-month running-mean trend line show strong seasonal variability and a pattern of interannual

variability, respectively (Fig. 2a). Both the seasonal and interannual dynamics of the NEB NDVI were directly influenced by the gradient between tropical North (5°N-25°N) and South Atlantic (5°S-25°S) (DIPOLE index). Figure 2 indicates the tropical Atlantic SSTs influence on the NDVI variability over the Brazilian semi-arid region. A visual inspection of the monthly NDVI NEB values in Figure 2a reveals the existence of multi-month episodes, which generally follow the negative and positive values of the tropical Atlantic Ocean DIPOLE over the entire period examined. Note that the general shape of the running mean trend line throughout the period is characterized by two major periods, the first being April 1984 through April 1991 (above monthly NDVI values of 0.5), and the second being January 1993 through November 1999 (below monthly NDVI values of 0.5). The overall upward and downward trends in vegetation greenness observed in Figure 2a show a dominant short-term oscillation of 7-8 year time scales superimposed with strong interannual oscillations. Regression analysis in the Figures (2b and 2c) was made by an examination of the two scatter plots through the monthly distribution of both, NDVI versus (represented as x-axis) the SSTs in the South Atlantic Ocean (represented as x-axis) (SATL) and North Atlantic Ocean (represented as x-axis) (NATL). The correlations between NDVI and SSTs are more pronounced in the tropical Atlantic Ocean than in the equatorial Pacific Ocean (linear regression analysis yielded a coefficient of determination of 0.0 and 0.14 for both the Niño-3.4 and Niño-3 indices) (not shown). Although a significant linear correlation between the NEB NDVI and the SATL-NATL Atlantic Ocean has been found (the 20-yr considered here is not long enough 30-yr, some aspects are noteworthy), this suggests that the question of whether or not the interannual relationships between the NEB NDVI and the Atlantic SSTs, and between the NEB NDVI and the ENSO signal operate independently.

To confirm the findings from Figure 2, the author divided the study years into two periods of nine years, 1982-1990 (upward trend in vegetation greenness) and 1991-1999 (downward trend in vegetation greenness). To assess whether the changes in the NEB NDVI values observed within these periods were related to the SSTs variability in the tropical Pacific and Atlantic Oceans, the author investigated correlations fields based on the links between February-May SST fields and February-May NEB NDVI time series, as well as February-May SST and February-May wind field differences between the 1980's and the 1990's (Fig. 4).

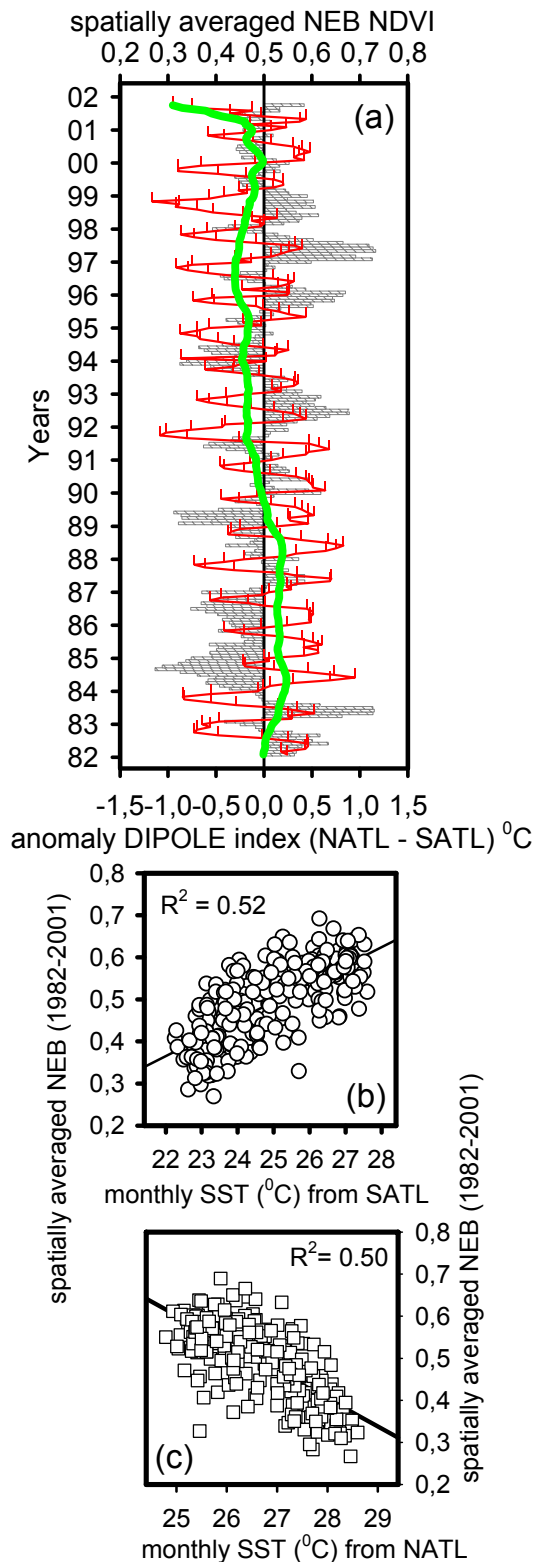


Fig. 2. Comparison (a) of the monthly NEB NDVI (red line) and its 36-month running-mean trend line (green line), and the anomaly DIPOLE index time series (anomaly NATL – anomaly SATL) (gray bar) for the period 1982-2001. Relationships between monthly NEB NDVI averaged over the entire NEB and monthly SST values from (b) South Atlantic (SATL) and (c) North Atlantic (NATL) for the period 1982-2001.

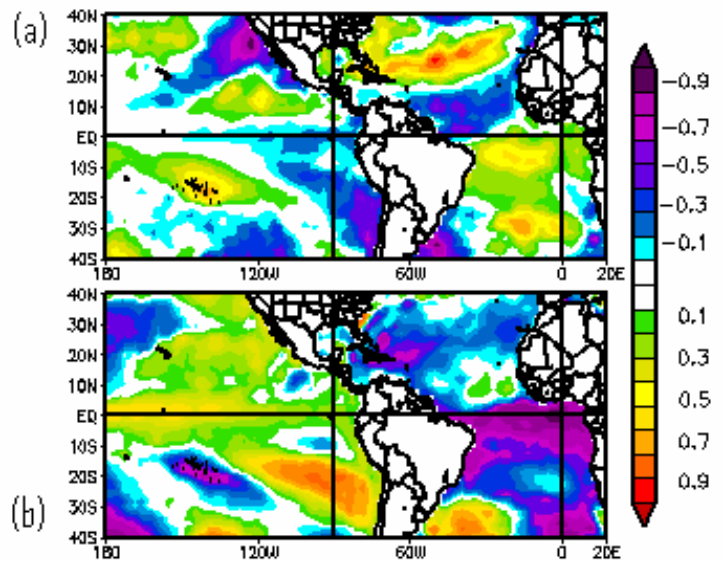


Fig. 3. Linear correlation fields between February-May SST and February-May NEB NDVI time series over the (a) 1980's and 1990's (b).

Figure 3 displays the differences between the correlation fields for the 1980's and the 1990's. Over the tropical Atlantic, Figure 3a and Figure 3b show two regions with an inverse relationship, may better explain how the tropical Atlantic SSTs affect NDVI (and therefore precipitation) throughout the February-May period 1980's. The zones with yellow-orange shading (significant positive correlations) where SSTs (not shown) are warmer than the 1990's and blue shading (significant negative correlations) where SSTs are cooler than 1990's. In general, cool ocean water upwind in the SATL leads to drought and reduced land plant growth, while warm SSTs produce excess rainfall and vigorous plant growth. For instance in Figure 3a, the opposite signs of the positive correlation (+0.5) in the zone centered between 3°S-10°S and 5°W-36°W, and the negative correlation (-0.6) in the zone centered between 17°N-EQ and 37°W-50°W, confirmed that there is a negative gradient (SATL warmer than NATL) (not shown) that brought rain (high plant growth over the Brazilian semi-arid throughout the February-May period 1980's). Studies refer to the gradient between the two seemingly unrelated regions as a "dipole" in the climate research. Over the Pacific Ocean, Figure 3a also reveals anomalous cluster tracks similar to those of opposite signs shown in the Atlantic Ocean. These cluster tracks are indicated by the alternating negative (-0.6), negative (-0.4), positive (+0.5), and negative correlations (-0.7) that extend from the coastal regions from the southernmost locations of South America (30°S-78°W) into the

Southwestern United States (30°N - 120°W). Note also that the occurrence of these cluster tracks in the tropical Atlantic Ocean is more pronounced than in the Pacific Ocean. These anomalous cluster patterns are co-located with the dipole variability in this region. Thus, the four correlation zones that define the cluster tracks are just the opposite signs of the tropical Pacific Ocean.

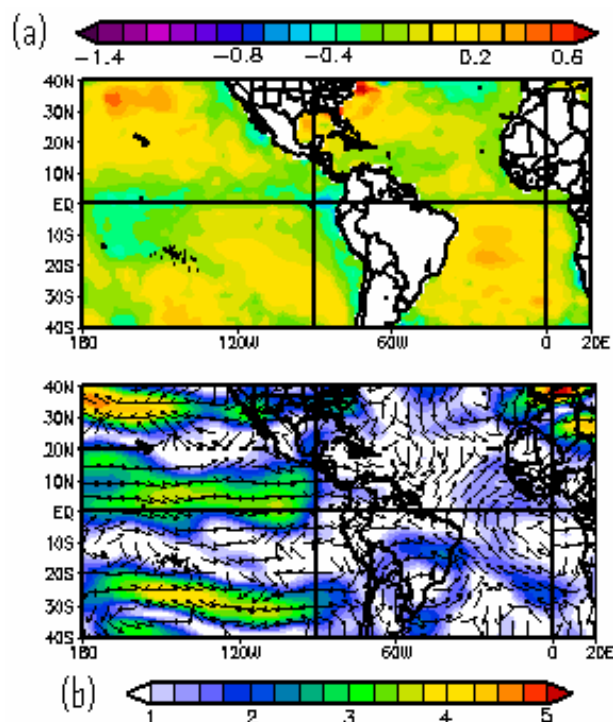


Fig. 4. February-May SST (a) and February-May wind at level of 200 hPa (b) field differences between the 1980's and the 1990's.

The results from the correlation fields observed in the Figure 3 do suggest ENSO signal exerted smaller influence on vegetation greenness throughout the February-May period 1980's than the 1990's over the NEB. However, the correlations for both periods were strong along the coast of California, where ENSO signal is an extensive source of rain in the Mojave Desert region (Cayan et al., 1999). Figure 3b displays the distribution of tropical Pacific SST-NDVI correlations are almost opposite to the tropical Atlantic. The central tropical Pacific displays positive correlations, with maximum correlations (from +0.4 to +0.8 values) confined to the zone centered between 13°S - 35°S and 80°W - 130°W . Negative correlations (from -0.4 to -0.8 values) occur in the entire tropical South Atlantic and mid-North Atlantic. Figure 3b also exhibits positive correlations in the equatorial North Atlantic, with maximum correlations (+0.2) found around the perimeter of the Western Africa along 10°N .

Positive and negative correlations in the East Pacific and North Atlantic key areas are consistent and correspond with the February-May SST field differences between the 1980's and 1990's, as well as February-May wind field differences between the 1980's and 1990's (Fig. 4). Although some biases exist, these field differences are adequate to justify interpretation of the SST-NDVI correlation fields for the two periods (1982-1990 and 1991-1999). Put together, the results shown in Figures 3 and 4 indicate that upper-level wind (200 hPa) fields may help sustain the influence of warm SSTs in the tropical Pacific and tropical Atlantic Oceans, at least for the NEB NDVI variability over the two periods studied. Figure 4b shows the upper level wind differences (at level of 200 hPa) between the period of 1982-1990 and the period of 1991-1999. Enhanced westerly flow is drawn in the Pacific Ocean from off the coast of North America, Central and South America along 35°N , 10°N , and 25°S , respectively. The northwesterly wind anomalies evolve along the eastern slopes of tropical and subtropical Andes and turn counter-clockwise around the Bolivia-high. The southwesterly wind anomalies interact with the sub-Saharan easterly jet. In addition to that, the Bolivian-high overall positioned near 19°S and 60°W is evident, which is a consequence of its strengthening.

5. DISCUSSION

Regional SST-dependent NEB NDVI modulation has been analyzed. The above results from the 20-year regional NDVI analysis suggest that the upward and downward trends in vegetation greenness over the last two decades of the 20th century might be attributed to the spatial-temporal impacts of the extreme rainfall variability (flooding and drought) on the NEB landscape in response to the tropical ocean SST anomalies (local SATL, remote NATL and remote ENSO signals). The reasonable but significant regional SST-NDVI correlations observed here do suggest that the two trends are modulated by fluctuations in SST of the nearby Atlantic (upward trend) and Pacific Oceans (downward trend). It was also revealed that upper-level (200 hPa) wind fields may exert a considerable influence on vegetation greenness on the NEB landscape, which is triggered by the SST anomalies in the tropical North Atlantic and equatorial Pacific Oceans. Finally, this study has suggested that an ocean-atmosphere observing system over the Atlantic Ocean must go beyond the equatorial region to be functional for seasonal climatic forecasting, at least for the NEB vegetation growing season.

References

- Alves, I.M.B., Repelli, C.A., 1992. Rainfall variation in the northern part of the Brazilian Northeast and the El Niño events-Southern Oscillation (ENSO), Brazilian Agrometeorological Magazine (Revista Brasileira de Agrometeorologia). São Paulo 7, 583-592.
- Azzali, S., Menenti, M., 2000. Mapping vegetation-soil-climate complexes in southern Africa using temporal Fourier analysis of NOAA-AVHRR NDVI data. *International Journal of Remote Sensing* 21, 973-996.
- Barbosa, H.A., 1998. Spatial and temporal analysis of vegetation index derived from AVHRR-NOAA and rainfall over Northeastern Brazil during 1982-1985. Master degree dissertation in Remote Sensing [in Portuguese]. Divisão de Sensoriamento Remoto, Instituto Nacional de Pesquisas Espaciais, São José dos Campos-SP, Brazil.
- Barbosa, H.A., 2004. Vegetation dynamics over the Northeast region of Brazil and their connections with climate variability during the last two decades of the twentieth century. Doctoral degree dissertation in Soil, Water, and Environmental Science at the University of Arizona. Tucson, Arizona.
- Barbosa, H., Huete, A., Baethgen, W. E. 2006. A 20-year study of NDVI variability over the Northeast Region of Brazil. *Journal of Arid Environments* (in press).
- Cayan, D., Redmond, K., Riddle, L., 1999. ENSO and hidrologic extremes in the Western United States, *Journal of Climate* 12, 2881-2893.
- Cramer, W., Fischer, A., 1996. Data requirements for global terrestrial ecosystem modeling, in B. Walker and W. Steffen (Eds.), *Global Change and Terrestrial Ecosystems*, Cambridge University Press, Cambridge, UK, pp. 529-565.
- Curran, P.J., 1980. Multispectral Photographic Remote Sensing of Vegetation Amount and Productivity. In *Proceedings of the Fourteenth International Symposium on Remote Sensing of the Environment*, Ann Arbor, MI, pp. 623-637.
- Dessay, N., Laurent, H., Machado, L.A.T., Shimabukuro, Y.E., Batista, G.T., Diedhiou, Ronchail, A., 2004. Comparative study of the 1982-1983 and 1997-1998 El Niño events over different types of vegetation in South America. *International Journal of Remote Sensing* 25, 4063 – 4077.
- Hulme, M., 2001. Climatic perspectives on Sahelian desiccation: 1973-1998. *Global Environmental Change* 11, 19-29.
- Moura, D., Shukla, J. 1981. On the dynamics of droughts in northeast Brazil: observations, theory, and numerical experiments with a general circulation model. *Journal of Atmospheric Science* 38, 2653-2675.
- Nicholson, S.E., Davenport, M.L., Malo, A.R., 1990. A comparison of the vegetation response to rainfall in the Sahel and East Africa, using normalized difference vegetation index from NOAA AVHRR, *Climatic Change* 17, 209-241.